THE EFFECT OF PATCH SIZE ON GRAIN-SCALE ROUGHNESS PARAMETERIZATION IN FLUVIAL ENVIRONMENTS

JANE GROOM(1), STEPHANE BERTIN(1) & HEIDE FRIEDRICH(1)

(1) Department of Civil and Environmental Engineering, University of Auckland, Auckland, New Zealand
E-mail: jgro800@aucklanduni.ac.nz

ABSTRACT

Several disciplines use the term roughness with little clarity. Although there is a general consensus that surface roughness is synonymous of the topography (or structure) of a surface. In fluvial environments, roughness is important due to the interactions between sediment, flow and ecology. River roughness is affected by the surface morphology, composition and structure, acting at different scales superimposed onto one another. There can also be confusion between the term roughness and flow resistance. It is important to differentiate between the two terms and ensure roughness is used as an input parameter for flow resistance equations, rather than a synonymous term. We use the term grain-scale roughness to describe the microtopography of a surface, therefore representing the topography as a result of individual grains. Detailed measurements of the surface were gathered through the collection of digital elevation models (DEMs) of patch-scale fluvial surfaces both in the laboratory and the field, obtained using stereo-photogrammetry. Moving-window detrending applied to the DEMs allowed isolating grain-scale roughness from the underlying larger-scale bedforms. Grain-scale roughness of the gravel patches was derived from the detrended DEMs using a series of surface metrics including skewness, kurtosis, standard deviation, inclination index (degree of imbrication) and roughness lengths obtained from second-order structure functions. These metrics (or roughness parameters) each represent different attributes of the surface. The data presented highlights the spatial variability of grain-roughness parameters at the patch-scale, indicating for a true representation of roughness, an adequate patch size for the surface must be obtained. Due to surface complexity, it can be concluded that a single roughness parameter cannot adequately describe roughness across a surface, even at the patch-scale. Developments to roughness parameterization are still required, however a more defined use of the term is available in the patch-scale fluvial application.

Keywords: Roughness / Parameterization / Scales / Microtopography / Fluvial

1 INTRODUCTION

Roughness is a term used in the literature throughout a variety of disciplines, however questions have been raised over the issue of whether we know the true meaning of roughness (Morvan et al., 2008; Lane, 2005). The importance of considering surface roughness is frequently stated, alongside ways of measuring and quantifying roughness. Yet, often research uses the term roughness with no clear definition within the context. Although previous authors have suggested there is a need to re-evaluate the meaning of roughness, recent reviews have stated this has not occurred (Lane, 2005; Powell, 2014). Therefore, it seems there is a call for a review in order to take a step back and define the term, rather than focusing on the progression of research in the application of surface roughness.

1.1 Defining the roughness term

Roughness is discussed in disciplines ranging from engineering to medicinal applications. For example, research has shown that surface roughness has an influence on the interaction between light beams hitting a surface, the electrical performance of a semiconductor device and a biological cell (Amaral et al. 2002; Lonardo et al. 2002). Biomedical research into surface roughness found a correlation between the surface roughness of cells and the RNA production, suggesting cell morphology and cell processes are sensitive to the microtopography of the cell (Martin et al., 1995). Although not defined outright, the authors indicate that surface roughness relates to the texture of the cell and use the term microtopography as a synonym for surface roughness (Martin et al., 1995). An increase in surface roughness has been found to increase the adhesive strength of ice, in the context of snow removal from road surfaces (Perez et al., 2015). Therefore, roughness is related to the topography of the surface, and is a physical property of the surface of interest. The performance of ships in the water is also related to surface roughness, as increased friction can result from changes to the surface topography, such as corrosion or paint cracking (Amaral et al., 2012). Finally, surface roughness plays an important role in the replacement of bones or joints in the human body. Surface topography of implants or

joint replacements influence the life-span and resistance, which is important due to the expense of joint or bone replacements (Lonardo et al., 2002).

Throughout different disciplines, authors have identified issues with quantifying roughness, as it is argued that surfaces are complex, which cannot be measured by a single parameter and roughness values are dependent on the scale of measurement (Lonardo et al., 1996; Amaral et al., 2012). These issues are present across disciplines, including Earth sciences and fluvial research (Smith 2014).

In Earth sciences, roughness has been used to represent a surface property, property of flow or in calibration models; however the differences between these applications are infrequently distinguished (Smith, 2014). Areas of Earth sciences which consider surface roughness include, but are not limited to: glaciers, flooding, catchment processes, tectonic activity, aeolian processes, meteorology and ecosystems. A recent review aimed to increase the clarity of the definition of roughness, and throughout the review the applied definition of roughness was the vertical range of sampled elevations and the variability or irregularity of this; thereby surface roughness is a parameter of topography (Smith, 2014).

1.2 Roughness in fluvial environments

Roughness is an important aspect within a fluvial system due to its influence on flow properties (including velocity and turbulence), sediment transport and local ecology (Aberle and Nikora, 2006; Hodge et al., 2009; Baewert et al., 2014; Curran and Waters, 2014). Estimations of roughness are important inputs for hydraulic and morphological models, along with models to determine the flow resistance within a channel (Tuijnder and Ribberink, 2012; Aberle and Smart, 2003). There are multiple scales of roughness which result from individual grains (grain-scale roughness) and larger bedform features, such as pebble clusters, which result in bedform roughness (Fig. 1); together contributing to the overall surface roughness of the river bed (Smart et al., 2004; Mao et al., 2011; Aberle et al., 2010; Tuijnder and Ribberink, 2012). Dependent on the scale of measurement, the roughness taken into consideration can vary (Morvan et al., 2008; Lane, 2005).

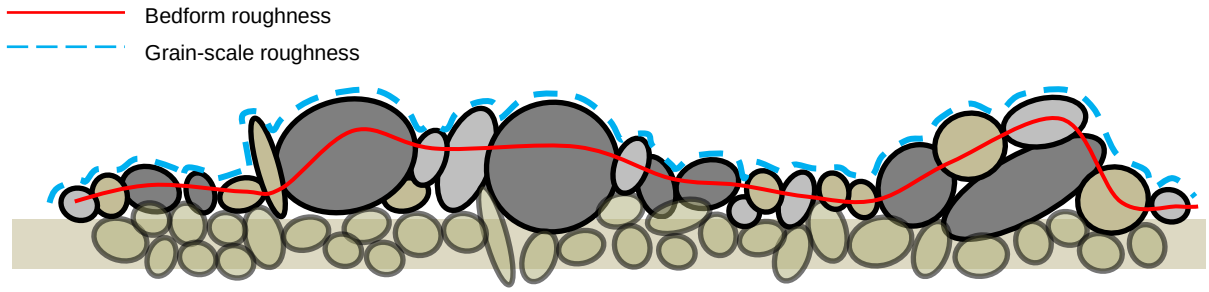

Figure 1. Schematic of the differences between grain-scale roughness (microtopography); resulting from individual grains, shown by the blue dashed line and the bedform roughness shown by the red line; reflecting larger scale humps and hollows (bed undulations) in the surface armor layer.

Generally in fluvial research, grain-scale roughness is used inter-changeably with bed microtopography (Smith, 2014). Recently there has been a move away from using the grain-size distribution of the surface sediment to the use of standard deviation of bed elevations to represent surface roughness. This is possible due to research using a random field of bed elevation approach, resulting in high-resolution 3D digital elevation models (DEMs) of the fluvial surface the size of a sediment patch (Mao et al., 2011; Bertin and Friedrich, 2014). Statistical analysis of patch-scale DEMs includes calculating probability distribution functions (including parameters, such as the standard deviation of elevations, skewness and kurtosis) and second-order structure functions. These surface metrics can provide indications of roughness resulting from larger form-scale features such as pebble clusters and can provide an indication of changes in roughness resulting from coarsening of the bed during the armoring process (Bertin and Friedrich, 2014; Qin and Ng, 2012; Coleman et al., 2011).

Several studies have found a linear relationship between certain percentiles of grain size (D_{50}, D_{84}, D_{90}) and the standard deviation of elevations from DEMs (Aberle and Nikora, 2006; Curran and Waters, 2014; Smart et al., 2004; Hodge et al., 2009). However, it should be noted that standard deviation, and therefore roughness, is not only affected by grain size, resulting in no unique relationship between the two; due to variations in packing, burial and imbrication of particles (Mao et al., 2011; Hodge et al., 2009; Powell, 2014). Some research argues that due to the relationship between the two, grain size is still an adequate measure of roughness (Schneider et al., 2015), although most research will now use standard deviation of elevation as an effective roughness parameter (Aberle et al., 2010; Baewert et al., 2014; Aberle and Smart, 2003). However, it is argued that using a single parameter to represent roughness will not be a holistic representation of the overall roughness of the bed, and is likely to underestimate the true roughness (Schneider et al., 2015; Morvan et al., 2008; Powell, 2014).

Following clarification of the roughness terminology, and adopting the definition of roughness equating to the microtopography of the surface; this study investigates the effect of patch size (in other words measurement size) on grain-scale roughness parameters obtained during analysis.

2 METHODOLOGY

2.1 Generating Digital Elevation Models (DEMs)

The microtopography of multiple gravel-bed patches, from both the field and the laboratory are represented by DEMs. Three field patches were collected from the Whakatiwai River in August 2014; which is a small gravel-bed stream in New Zealand. This data is presented in Bertin and Friedrich (2016), and here makes up the surfaces labelled FIELD_1 – FIELD_3, with numbers increasing with distance upstream. Patches were taken on different gravel bars, which differed in sediment size and the structure of the surface. Patches chosen were located on the water edge at the bar head, to ensure water-working and providing consistency in the measurements taken.

Surfaces formed in the laboratory were armored beds resulting from a flow rate of 84L/s (mean flow velocity = 0.82 m/s, shear velocity = 0.077 m/s and uniform water depth = 0.225 m), until the sediment transport rate dropped below 1% of the initial transport rate, when under the condition of sediment starvation. Experimental surfaces formed in a 19 m long, 0.45 m wide and 0.5 m deep non-recirculating flume, set to a slope of 0.5%. Differing bimodal sediment mixtures were used, ranging in size from 0.7 mm to 35 mm. The first sediment mixture contained 85% gravel and 15% sand, compared to 91% gravel and 9% sand in the second sediment mixture. Three DEMs for each sediment size are presented, making a total of six laboratory DEMs (labelled SED1_T1-3 and SED2_T1-3).

A pair of consumable Nikon D5100s (16.4 Mpixel, 23.6 x 15.6 mm^2 sensor size) with Nikkor 20 mm lenses were vertically installed in stereo above the gravel patch of interest. Two overlapping images, or stereo photographs, are used to produce DEMs through the following method. Firstly, calibration was completed using the method of Zhang (, 2000), whereby several stereo photographs of a chequerboard are taken, and using Bouguet (2010)'s calibration toolbox in Matlab®, intrinsic (i.e. camera) and extrinsic (i.e. setup) calibration parameters are obtained. Images are then accurately rectified (with a maximum error < 1 pixel) using the calibration data, whereby corresponding pixels between overlapping images are ideally on a same scanline. Stereo-matching is completed using Gimel'farb (, 2002)'s symmetric dynamic programming stereo (SDPS) algorithm, which produces point cloud data and ortho-images. Point clouds were interpolated onto regular grids with a 1 mm spacing, which reduces bias from non-uniform data when calculating surface metrics such as the standard deviation of elevations (Hodge et al. 2009a). Outliers were identified using the mean elevation difference parameter and replaced using bi-cubic spline interpolation (Hodge et al. 2009a), before DEMs were normalized to have a mean bed level of zero and rotated to align in the flow direction; which for the field data was determined by eye based on observations of the channel and grain imbrication (Laronne and Carson, 1976; Millane et al., 2006; Bertin and Friedrich, 2016).

Finally, prior to the calculation of surface metrics, a moving-window detrending strategy (Smart et al., 2002; Hodge et al., 2009) was applied to all DEMs. This removed large-scale distortions in the surface, which included those larger than the cluster size; such as hollows and bumps. Following the method of Smart et al. (2002), the trend surface was estimated over a grid with point spacing 1.25 × D_{90A} (where D_{90A} is the D_{90} of the surface material), with the elevation of grid points measured by averaging DEM data points within a circle of diameter 2.5 × D_{90A} centered on the grid point, and removed from the measured DEMs before analysis. This way, data analysis could focus on the grain topography and the properties determined from the detrended DEMs were linked to grain-scale roughness.

2.2. Measuring the surface grain size

In order to compare the topographic information derived from DEMs with sediment size, the intermediate (b-) axis of grains was determined for each patch. Here D_{50A} is used to represent the median grain size of the armor surface, for which 50% is smaller by weight; as the armored surface differs from the bulk mixture of the bed. Single, vertical images, containing over 400 detectable grains, were used in the image-analysis tool Basegrain®, whereby automatic grain separation and Fehr (1987)'s line-sampling method are applied for analysis (Detert and Weitbrecht, 2012). Grain sieving was completed on the sediment mixtures from the laboratory in order to determine particle shape, specific gravity and the sediment grading curves.

2.3 Calculating surface metrics for grain-roughness parameterization

A total of six surface metrics were calculated in order to assess the effect of DEM size on grain-roughness parameters. Using a moving-window analysis technique, the size of the moving window is indicative of DEM size. Surface metrics were calculated for square windows moving across detrended DEMs, for different window sizes. A large overlap (up to 95%) between moving windows ensured robust statistics even at large window sizes. All window sizes were made proportional to the surface D_{50A} (i.e. calculations were made within windows proportional to the population median grain size determined over the whole DEM). Due to the nature of the

DEMs being rectangular in shape, square moving windows were chosen to calculate roughness parameters; in contrast to the circular moving windows used by Scown et al. (2015). The maximum window size for analysis varied between 12 x D_{50A} (i.e. a window size of 12 times the surface D_{50} along both x and y directions) and 26 x D_{50A} due to the differences in DEM areas and bed structure (e.g. sediment size). For clarity, a single value for DEM size normalized by D_{50A} will be used herein, reflecting the dimensions of the DEM in both the x and y directions.

The surface metrics calculated from DEMs are the standard deviation σ_Z, Skewness S_K, Kurtosis K_u, horizontal roughness lengths in both streamwise and cross-stream directions (L_x and L_y), and the inclination index in the flow direction *I0.* Surface metrics including σ_Z, S_K and K_u (Eq. 1) are determined from probability distribution functions (PDFs) and have been used in several studies as characteristics of bed roughness (Aberle and Nikora, 2006; Scown et al. 2015). The roughness parameter most used in flow resistance equations is σ_Z, as it represents the vertical roughness length of a surface (Aberle and Smart, 2003; Noss and Lorke, 2016). The degree of water-working can be gathered from the S_K (degree of asymmetry of PDF), where positive values suggest a water-worked surface whereby fine grains have filled surface depressions, and therefore have reduced the magnitudes of surface deviations below the mean (Aberle and Nikora, 2006). Finally, K_u measures the regularity of the bed, whereby a large kurtosis value (heavy tails and narrow peak distribution) is a result of variance from irregular, extreme deviations. Lower kurtosis values are a result of deviations from the mean occurring frequently; indicating a uniform and compact distribution of the surface (Coleman et al. 2011).

$$\sigma_Z{}^2 = \frac{1}{N'}\sum_{i=1}^{N'}(z_i - \langle z_i \rangle)^2$$

$$S_K = \frac{1}{N'\sigma_Z{}^3}\sum_{i=1}^{N'}(z_i - \langle z_i \rangle)^3$$

$$K_u = \left[\frac{1}{N'\sigma_Z{}^4}\sum_{i=1}^{N'}(z_i - \langle z_i \rangle)^4\right] - 3 \qquad [1]$$

where, z represents the bed elevation at location (x,y) in a DEM, N' is the total number of DEM points and < > represents the mean value.

Horizontal roughness lengths in both the streamwise and the cross-stream direction (L_x and L_y, respectively) are scaling characteristics of a surface and are calculated from second-order structure functions (Eq. 2 & Fig. 2):

$$D_{G2}(\Delta x, \Delta y) = \frac{1}{(N-n)(M-m)}\sum_{i=0}^{N-n}\sum_{j=0}^{M-m}\{\left|z(x_i + n\delta x, y_j + m\delta y) - z(x_i, y_j)\right|\}^2 \qquad [2]$$

where, $\Delta x = n\delta x$ and $\Delta y = m\delta y$; δx and δy are the sampling intervals (i.e. DEM resolution) in the longitudinal and transverse directions respectively; n=1,2,3,…N and m=1,2,3,…M. N and M are the number of DEM points in the same two directions.

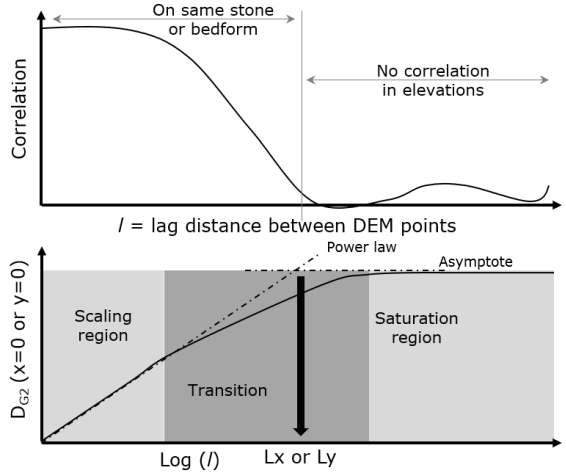

Figure 2. Typical gravel-bed elevation correlation and structure function graph for different spatial lags, used to determine horizontal roughness lengths L_x and L_y. Adapted from Smart et al. (2002).

Structure functions are used to measure changes in elevation correlations at different spatial lags and in different directions (Fig. 2). Here (because of detrending), small values are indicative of areas of similar elevations; suggesting DEM points are on the same grain, whilst larger values suggest surface elevations are no longer correlated and therefore are not of the same grain. Structure functions for gravel-beds have three regions (Fig. 2); a scaling region with uniform slope at small lags, a saturation region at large lags, where the slope is zero, with a transition region in between, where the slope decreases (Nikora et al., 1998; Hodge et al., 2009). The scaling region of structure functions provides the horizontal roughness lengths from the slope breakpoint (Fig. 2), located at the intersection between the tangent to the scaling region slope and the saturation level asymptote, in both x and y directions (Nikora et al., 1998). The maximum spatial lags for calculating grain-roughness lengths were chosen to be half the window size in both directions.

The inclination index *I0* in the flow direction is calculated using Eq. 3 (Smart et al., 2004). The inclination index is the difference between the fraction of positive and negative inclinations of particles, divided by the total number of positive, negative and zero inclinations at a given lag distance, equal to the resolution of the DEM. Positive slopes are counted as elevation increases with the downstream direction.

$$I0 = \frac{n_+ - n_-}{Ns} \quad [3]$$

where, n_+ and n_- are the number of positive and negative slopes between successive DEM points, respectively, and Ns is the total number of slopes.

Unreliable slope values of below 0.01 were not counted in the numerator of Eq.3 (Millane et al., 2006). Positive inclination index values reflect a predominance of positive slopes in the flow direction, which is the sign of particle imbrication (Laronne and Carson, 1976; Millane et al., 2006). Parameterizing grain imbrication in this manner is informative of the flow direction forming the bed surface; providing insights into both the bed stability and flows that created the surface.

Finally, the variability of the surface was quantified using the coefficient of variation (CV), which is calculated as the standard deviation of the grain-roughness property determined over all moving windows, divided by the mean, and expressed as a percentage. This was completed on all six surface metrics, providing the values were positive; therefore it could not be completed for all DEM sizes considered (particularly the case S_k and *I0).* Furthermore, the error in σ_z is calculated in order to quantify surface variability. This was completed by calculating the relative difference between each moving-window σ_z and the population σ_z, averaged over all moving windows of the same size, and expressed as a percentage.

3 RESULTS

Roughness parameters for nine DEMs were plotted as boxplots (except for CV, which was plotted as a line graph) in order to visualize the variability in statistics for changing DEM size, using the moving-window analysis technique. Figure 3 presents an example of these boxplots for SED1_T1; which is a laboratory DEM. Plateaus in statistics were observable when the median values stabilized and variability of roughness statistics (e.g. boxplot whiskers) remain similar across increases to DEM size. These plateaus were confirmed statistically with 95% confidence intervals and a paired t-test. As can be seen in Figure 3, and observed across all DEMs studied, an increase in DEM size (and therefore patch size) results in a decrease in the variance of roughness statistics generated across the surface; suggesting at these sizes the patch size is adequate to obtain a representative roughness statistic of the bed surface. At small DEM sizes, the variability is large and therefore statistics obtained from DEMs of this size would be non-representative of the surface topography. Figure 3 shows for this laboratory DEM (SED1_T1) variability plateaus at 14 x D_{50A} for all roughness parameters, with σ_z appearing to have the largest variability at the larger DEM sizes.

Plateaus in statistics were observed in the majority of the DEMs, for multiple roughness parameters. These are summarized in Table I below. Generally, for field DEMs, once the DEM size exceeds 16-18 x D_{50A} the roughness statistics are deemed to provide a representative indication of surface roughness, with little effect of inherent surface variability. These plateaus appeared slightly earlier in laboratory DEMs, with plateaus between 14-16 x D_{50A}. It is worth noting that not all roughness parameters displayed evidence of a threshold, from both field and laboratory settings (indicated in Table I by a dash [-]). Noticeably, FIELD_2 evidenced plateaus at lower DEM sizes of 10 x D_{50A}.

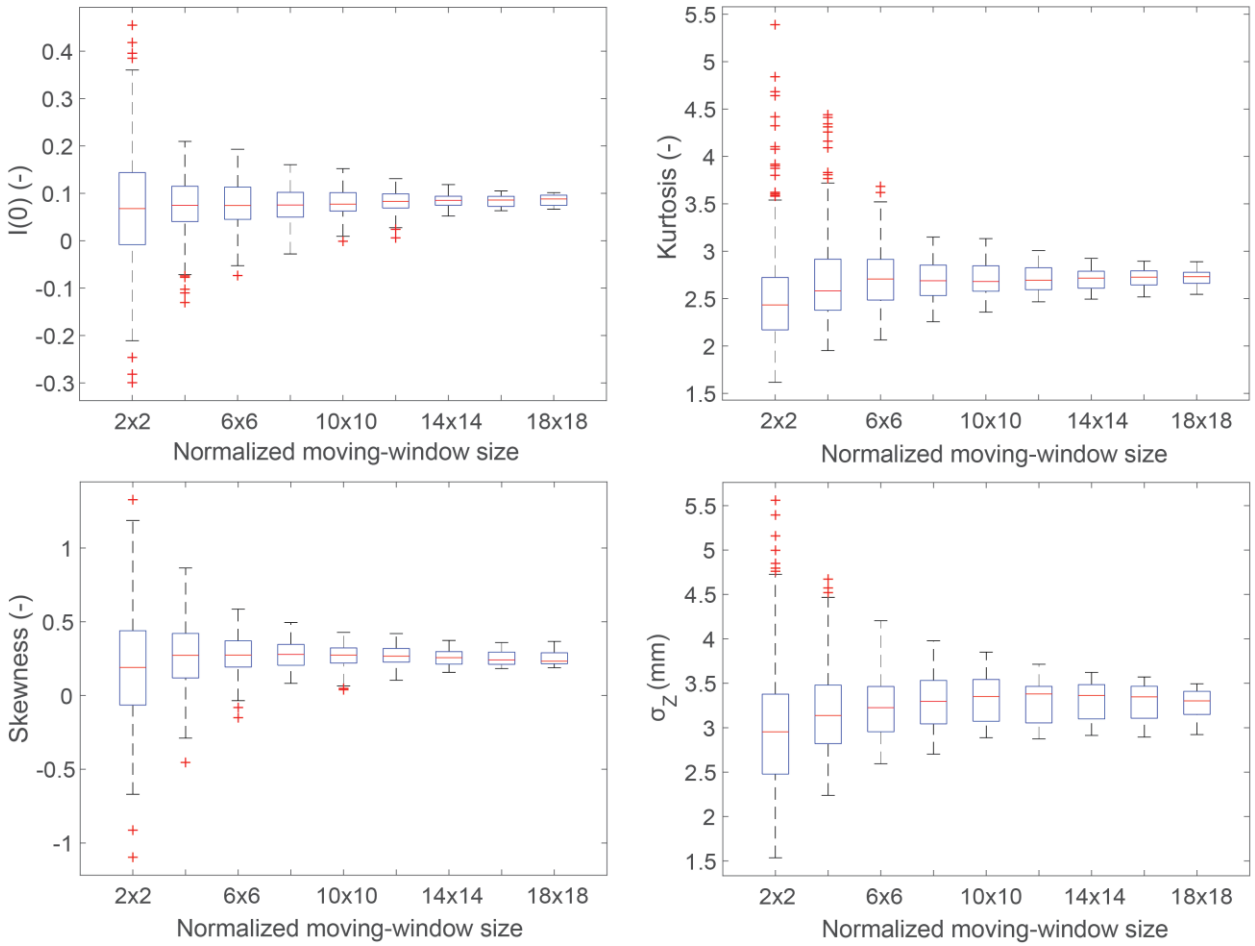

Figure 3. Boxplots of roughness statistics for SED1_T1 laboratory DEM, calculated at different moving-window sizes normalized in both directions by D_{50A}; showing plateaus in statistics with an increase in DEM size (e.g. at 14 x D_{50A}).

Table I: Summary table showing plateau values, representing the minimum DEM size (normalized by D_{50A} in both x and y directions) to consider for grain-roughness properties representative of the surface, whereby the mean of the roughness parameter stabilizes and variability is minimum for all nine DEMs studied; from both laboratory and field. The second column provides the D_{50A} value (in mm) for reference.

DEM name	Location	D_{50A} (mm)	CV	I0	Ku	Sk	σ_z
FIELD_1	Field	18.7	18	14	18	16	20
FIELD_2	Field	47.2	-	10	10	10	-
FIELD_3	Field	19.4	18	12	18	16	18
SED1_T1	Lab	18.0	14	14	14	14	14
SED1_T2	Lab	19.0	14	12	-	14	14
SED1_T3	Lab	18.5	12	14	16	16	14
SED2_T1	Lab	19.5	-	12	14	-	14
SED2_T2	Lab	17.5	12	10	16	16	14
SED2_T3	Lab	18.5	16	14	16	16	-

The error in σ_z for each window size was plotted for each DEM to present the effect of DEM size on all data studied in this paper. Figure 4 presents the error for all nine DEMS over a range of DEM sizes normalized by D_{50A}. At smaller DEM sizes, the error in σ_z is high for all DEMs (> 15%), with field data displaying the highest values (between 25% and 35%). There is a wider spread in the variability of error values across all DEMs at smaller DEM sizes, however as DEM size increases, the error values decrease (namely below 10% at 14 x D_{50A}) and the variability of error values reduces. Note that Figure 4 is restricted to 18 x D_{50A}, as following this DEM size, only a few data points are available (e.g. for FIELD_1 and FIELD_3). Further note that for 14 – 18 x D_{50A} there is one less data point, due to FIELD_2 being limited to a size of 12 x D_{50A}.

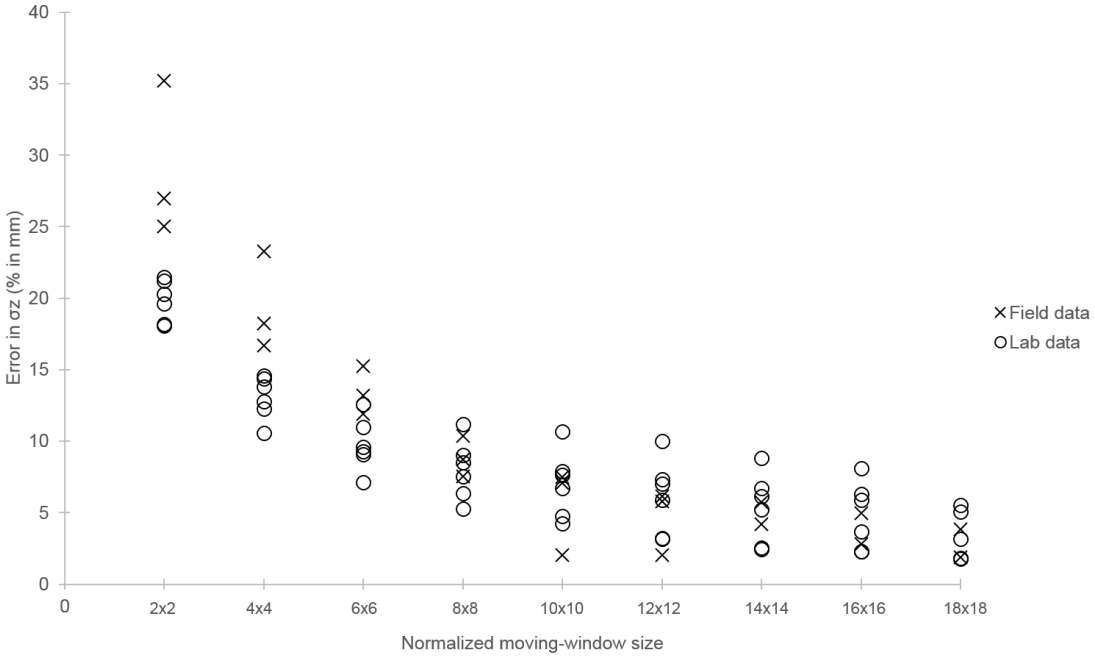

Figure 4. Scatter plot of all nine DEMs showing the error in σ_z (expressed as a percentage) calculated at different moving-window sizes normalized in both directions by D_{50A}. Circular markers represent laboratory data, compared to markers with a cross which are the field data. The presentation of data is limited to 18 x D_{50A}, as only a few DEMs provide data exceeding this size. Note there are only two field data points from 14 x D_{50A}, due to FIELD_2 only reaching 12 x D_{50A}.

4 DISCUSSION

Decreases in the variability of statistics were not only seen visually in boxplots (as in Figure 3), but there was a distinct decrease in CV with increases in DEM size. These findings are similar to a study which found an increase sampling density (and therefore spatial coverage) of measurements into bed shear stress and roughness lengths of a gravel-bed channel, were associated with a reduction in CV (Cienciala and Hassan, 2016). In contrast to this, a larger-scale floodplain investigation found an increase in CV with DEM size (Scown et al., 2015), likely due to the difference in scale of analysis in comparison to this study. It is therefore important to consider the scale of roughness under investigation; as mentioned previously, the incorporation of bedform roughness would be non-representative of grain-scale roughness or the microtopography of the surface. This study used a detrending method which aimed at removing the influence of bedform-scale roughness of the surfaces in order to gain solely grain-roughness properties. Isolating the different scales of roughness through a suitable detrending strategy is a key analytical decision which should be dependent on the required application.

Variability in roughness parameters does not completely reduce (Figure 4), as gravel-bed surfaces are non-uniform in nature. Differences in packing, burial, sorting, shape and size of sediment account for a lack of uniformity and contribute to the variability in topography seen across DEM surfaces (Graham et al., 2010). Often, individual roughness parameters display differing degrees of variability (Figure 3); therefore suggesting some parameters are more sensitive to surface variability in comparison to others. This would suggest using a single roughness parameter is inadequate to holistically represent the surface roughness of gravel-beds in fluvial environments.

Plateaus in statistics were taken to be when the median values stabilize and variability remains consistent with further increases to DEM size. Statistical confirmation of these plateaus were completed through 95% confidence intervals, which has previously been used to assess spatial variability in data sample size (Cienciala and Hassan 2016), and a paired t-test to assess for significant differences in the mean values of each DEM size. Both statistical methods were used, as variability could fluctuate whilst median values remained stable and visual observations from boxplots (as in Figure 3) considered both of these factors before a plateau was determined. Some roughness parameters did not display plateaus in statistics; likely due to the surface displaying high spatial variability and/or the maximum DEM size was inadequate to gain a representative statistic.

Differences in the plateaus between field and laboratory DEMs result from differences in the complexity of these surfaces. Whilst laboratory DEMs are reasonably uniform in nature (therefore less variability and lower plateaus), field surfaces were found to have more poorly sorted sediment (Bertin and Friedrich 2016), resulting in increased surface variability. In Table I, some of the field DEMs displayed plateaus at a smaller DEM size in comparison to the other DEMs. In particular this is the case for FIELD_2; likely due to the surface having a

larger D_{50A} (of 47 mm in comparison to ~ 20 – 25 mm) than other field DEMS. Previous investigations using this data identified a high number of imbricated grains, poorly sorted sediment and high σ_z values (Bertin & Friedrich 2016), highlighting differences between this patch and the other field data.

It can be gathered from Table I, that for both laboratory and field, DEMs would require a DEM with dimensions exceeding 16 x D_{50A} in both directions in order to provide representative roughness statistics. Although, it is important to note that the DEM size will be dependent on the scale of investigation for the application and also on the surface composition and morphology. Making the thresholds dimensionless by D_{50A} allow for easy comparison between surfaces and reduces the effects of differing grain sizes of each surface. However, although the work is dimensionless by D_{50A}, differences in microtopography may be as a result of other influences such as sediment shape, sorting and structural arrangement (Smart et al., 2002; Powell, 2014). Therefore surfaces with similar D_{50A} may provide different roughness properties; evidencing why using roughness parameters based on the topography of a surface is superior to using a simple grain size characteristic, as previously undertaken.

Figure 4 reinforces evidence of requiring an adequate DEM size for representative statistics; due to a reduction in error in σ_z with increases in DEM size. The error in σ_z reduces for all DEMs studied to below 10% from 14 x D_{50A} size. Following this DEM size, further increases in DEM size have a slight reduction in error in σ_z, however this is not as significant as increases from the small DEM sizes of 2 x D_{50A} for example. Therefore this would suggest there is a plateau across all DEMs for grain-scale roughness statistics becoming representative and with as small error values as possible.

The recommended DEM size in this study would appear lower than the value of 21 x D_{50} suggested as an appropriate patch size in previous literature (Ockelford and Haynes, 2013). Likely this is resulting from the sediment in this study being from the armor layer (D_{50A}), in comparison to the assumption that Ockelford and Haynes refer to the bulk mixture D_{50} (of 4.8 mm). Clarity in the literature between the D_{50} values obtained from the bulk sediment or armor layer (D_{50A}) is needed for universal comparisons. However differences in threshold values between studies highlight the importance of other surface properties such as sediment sorting. Furthermore, differences in these recommendations may result from different analytical methods used; for example this studied removed the effect of bedforms through a moving-window detrending method. Therefore smaller patch sizes may be indicative of the grain-scale roughness, compared to larger patch sizes required for surface incorporating bedform (or larger scale) roughness. Isolating the influence of these scales of roughness is an important consideration for the required application.

5 CONCLUSIONS

Firstly, clarification of the term roughness is presented, whereby the term grain-scale roughness is synonymous with the microtopography of a surface; resulting from individual grains. Larger scale roughness (such as bedform roughness) results from the clustering of particles and forming bed undulations across the surface. It is important to remove these larger scale roughness trends to obtain reflective grain-scale roughness.

There is a clear influence of patch size (e.g. DEM size) on the grain-scale roughness parameters obtained during analysis, with high variability in results using smaller patch sizes. This high variability is also reflected in larger error in σ_z at smaller DEM sizes, with reductions in values as DEM size increases. In order to produce representative grain-scale roughness parameters, a DEM size of > 14 x D_{50A} (in both directions) should be used, in both the laboratory and field; albeit larger patch sizes (16 – 18 x D_{50A}) are required for field surfaces. Differences between the patch size required in the laboratory and the field is likely due to differences in surface structure and composition (and therefore complexities) between the two environments. Therefore, adequately isolating different scales of roughness (e.g. through a sufficient detrending method) is essential to obtain representative grain-roughness values.

Finally, the variability expressed across surfaces highlights spatial variability in the microtopography; therefore using a single roughness parameter (such as the previously used σ_z) is not sufficient, and in order to holistically represent the surface complexity and grain-roughness, a combination of parameters, as used in this paper are required. Analysis was undertaken on data from both the laboratory and field environments with the similarities between the effect of patch size in both presented; therefore these trends observed can be generalized over multiple gravel patches in differing environments.

ACKNOWLEDGMENTS

The study was partly funded by the Marsden Fund (Grant No. UOA1412), administered by the Royal Society of New Zealand.

REFERENCES

Aberle, J. & Nikora, V. (2006). Statistical properties of armored gravel bed surfaces. *Water Resources Research,* 42, W11414, DOI: 10.1029/2005WR004674.

Aberle, J. & Smart, G. (2003). The influence of roughness structure on flow resistance on steep slopes. *Journal of Hydraulic Research,* 41, 259-269.

Aberle, J., Nikora, V., Henning, M., Ettmer, B. & Hentschel, B. (2010) Statistical characterization of bed roughness due to bed forms: A field study in the Elbe River at Aken, Germany. *Water Resources Research,* 46, W03521, DOI: 10.1029/2008WR007406.

Amaral, R., Chong, L.H. & Selvaduray, G. (2012). Surface roughness. *San Jose State University, http://www.sjsu.edu/faculty/selvaduray/page/papers/mate210/surface.pdf*

Baewert, H., Bimböse, M., Bryk, A., Rascher, E., Schmidt, K. and Morche, D. (2014). Roughness determination of coarse grained alpine river bed surfaces using Terrestrial Laser Scanning data. *Zeitschrift für Geomorphologie, Supplementary Issues,* 58, 81-95.

Bertin, S. & Friedrich, H. (2014). Measurement of gravel-bed topography: evaluation study applying statistical roughness analysis. *Journal of Hydraulic Engineering,* 140, 269-279.

Bertin, S. & Friedrich, H. (2016). Field application of close-range digital photogrammetry (CRDP) for grain-scale fluvial morphology studies. *Earth Surface Processes and Landforms*, DOI: 10.1002/esp.3906

Cienciala, P. & Hassan, M.A. (2016). Sampling variability in estimates of flow characteristics in coarse-bed channels: Effects of sample size. *Water Resources Research*, 52, 1899-1922.

Coleman, S.E., Nikora, V.I. & Aberle, J. (2011). Interpretation of alluvial beds through bed-elevation distribution moments. *Water Resources Research,* 47, W11505. DOI: 10.1029/2011WR010672

Curran, J.C. & Waters, K.A. (2014). The importance of bed sediment sand content for the structure of a static armor layer in a gravel bed river. *Journal of Geophysical Research: Earth Surface,* 119: 1484-1497.

Gimel'farb, G. (2002). Probabilistic regularisation and symmetry in binocular dynamic programming stereo. *Pattern Recognition Letters,* 23, 431-442.

Graham, D.J., Rollet, A., Piégay, H. & Rice, S.P. (2010). Maximizing the accuracy of image-based surface sediment sampling techniques. *Water Resources Research,* 46, W02508. DOI: 10.1029/2008WR006940

Hodge, R., Brasington, J. & Richards, K. (2009). Analysing laser-scanned digital terrain models of gravel bed surfaces: linking morphology to sediment transport processes and hydraulics. *Sedimentology,* 56, 2024-2043.

Lane, S.N. (2005). Roughness–time for a re-evaluation?. *Earth Surface Processes and Landforms,* 30, 251-253.

Laronne, J. & Carson, M. (1976). Interrelationships between bed morphology and bed-material transport for a small, gravel-bed channel. *Sedimentology,* 23, 67-85.

Lonardo, P., Lucca, D. & De Chiffre, L. (2002). Emerging trends in surface metrology. *CIRP Annals-Manufacturing Technology,* 51, 701-723.

Lonardo, P., Trumpold, H. & De Chiffre, L. (1996). Progress in 3D surface microtopography characterization. *CIRP Annals-Manufacturing Technology,* 45, 589-598.

Mao, L., Cooper, J.R. & Frostick, L.E. (2011). Grain size and topographical differences between static and mobile armour layers. *Earth Surface Processes and Landforms,* 36, 1321-1334.

Martin, J., Schwartz, Z., Hummert, T., Schraub, D., Simpson, J., Lankford, J., Dean, D., Cochran, D. & Boyan, B. (1995). Effect of titanium surface roughness on proliferation, differentiation, and protein synthesis of human osteoblast-like cells (MG63). *Journal of Biomedical Materials Research,* 29, 389-401.

Millane, R., Weir, M. & Smart, G. (2006). Automated analysis of imbrication and flow direction in alluvial sediments using laser-scan data. *Journal of Sedimentary Research,* 76, 1049-1055.

Morvan, H., Knight, D., Wright, N., Tang, X. & Crossley, A. (2008). The concept of roughness in fluvial hydraulics and its formulation in 1D, 2D and 3D numerical simulation models. *Journal of Hydraulic Research,* 46, 191-208.

Nikora, V.I., Goring, D.G. & Biggs, B.J. (1998). On gravel-bed roughness characterization. *Water Resources Research,* 34, 517-527.

Noss, C. & Lorke, A. (2016). Roughness, resistance, and dispersion: Relationships in small streams. *Water Resources Research,* 52, 2802-2821.

Ockelford, A. & Haynes, H. (2013). The impact of stress history on bed structure. *Earth Surface Processes and Landforms,* 38, 717-727.

Perez, A.P., Wåhlin, J. & Klein-Paste, A. (2015). Effect of surface roughness and chemistry on ice bonding to asphalt aggregates. *Cold Regions Science and Technology,* 120, 108-114.

Powell, D.M. (2014). Flow resistance in gravel-bed rivers: Progress in research. *Earth-Science Reviews,* 136, 301-338. DOI: http://dx.doi.org/10.1016/j.earscirev.2014.06.001

Qin, J. & Ng, S. (2012). Estimation of Effective Roughness for Water-Worked Gravel Surfaces. *Journal of Hydraulic Engineering,* 138, 923-934. DOI: 10.1061/(ASCE)HY.1943-7900.0000610

Schneider, J.M., Rickenmann, D., Turowski, J.M. & Kirchner, J.W. (2015). Self-adjustment of stream bed roughness and flow velocity in a steep mountain channel*. Water Resources Research,* 51, DOI: 10.1002/2015WR016934

Scown, M.W., Thoms, M.C. & De Jager, N.R. (2015). Measuring floodplain spatial patterns using continuous surface metrics at multiple scales*. Geomorphology* 245: 87-101.

Smart, G., Aberle, J., Duncan, M. & Walsh, J. (2004). Measurement and analysis of alluvial bed roughness*. Journal of Hydraulic Research,* 42, 227-237.

Smart, G.M., Duncan, M.J. & Walsh, J.M. (2002). Relatively rough flow resistance equations*. Journal of Hydraulic Engineering,* 128, 568-578.

Smith, M.W. (2014). Roughness in the Earth Sciences*. Earth-Science Reviews,* 136, 202-225. DOI: http://dx.doi.org/10.1016/j.earscirev.2014.05.016

Tuijnder, A.P. & Ribberink, J.S. (2012). Experimental observation and modelling of roughness variation due to supply-limited sediment transport in uni-directional flow*. Journal of Hydraulic Research,* 50, 506-520.

Zhang, Z. (2000). A flexible new technique for camera calibration*. IEEE Transactions on Pattern Analysis and Machine Intelligence,* 22, 1330-1334.